



MWC 645: A Puzzling FS CMa-type Star

Andrea Fabiana Torres

Facultad de Ciencias Astronómicas y Geofísicas, Universidad Nacional de La Plata and Instituto de Astrofísica de La Plata (CCT La Plata-CONICET, UNLP), La Plata, Argentina

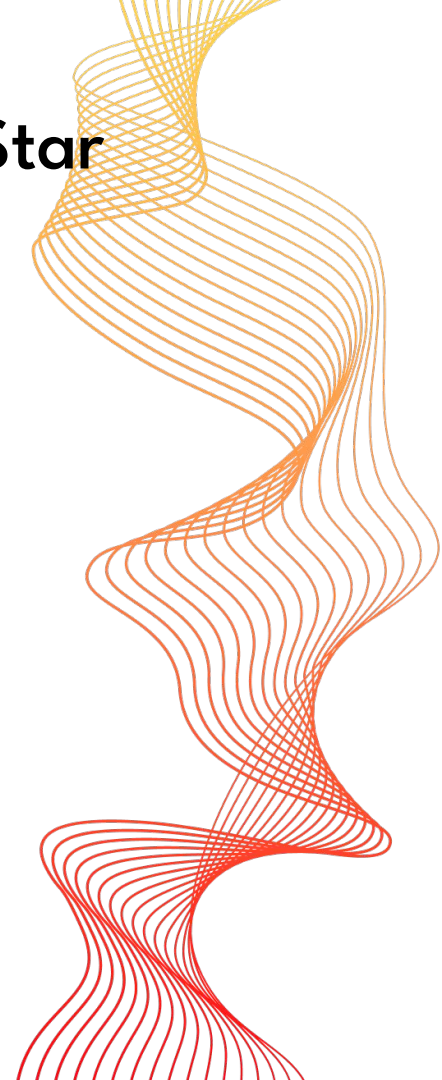
In collaboration with María Laura Arias, Michaela Kraus, Lorena Verónica Mercanti and Tõnis Eenmäe



Facultad de Ciencias
Astronómicas
y Geofísicas
UNIVERSIDAD NACIONAL DE LA PLATA



UNIVERSIDAD
NACIONAL
DE LA PLATA





Introduction

B-type stars exhibit peculiar phases that astrophysicists still struggle to understand.

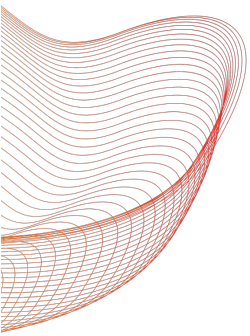
The **B[e] phenomenon** is one such phenomena not yet well understood.

Its manifestation involves:

- The presence of permitted and forbidden low-excitation emission lines of neutral and low ionization metals arising from circumstellar (CS) gas.
- The large infrared excess due to CS dust.

It is associated with:

- stars with different initial masses
- isolated or in binary systems
- in different evolutionary stages.





Introduction

A crucial factor:

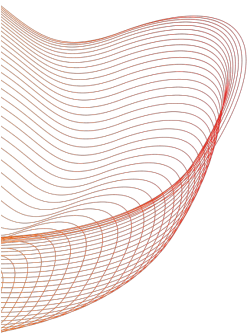
Despite the differences among the stars, the physical conditions of their CS gaseous and dusty envelopes are similar.



The photospheric features of B[e] stars are veiled by the CS envelopes, making classification challenging.

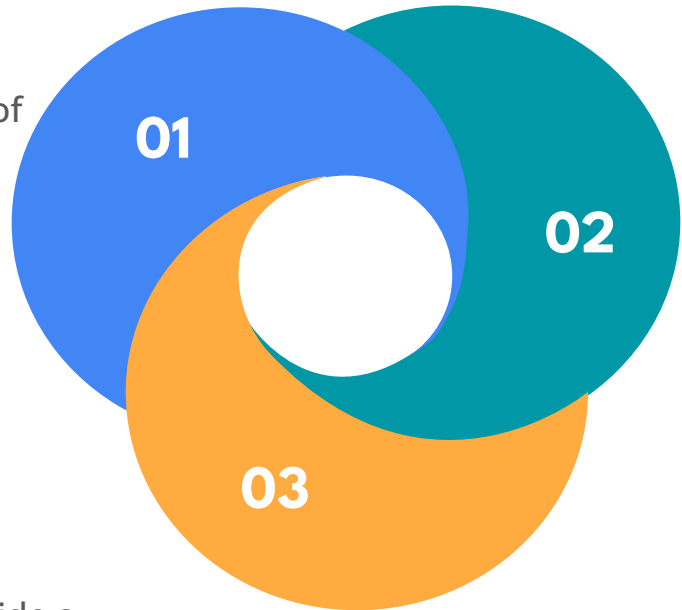
→ “**UnclB[e]** stars” (Lamers et al., 1998).

Miroshnichenko (2007) proposed a new group: **FS CMa** stars.



FS CMa Stars: Observational Defining Criteria

The presence of a hot star continuum with emission lines of H I, Fe II, O I, [Fe II], [O I], Ca II.



An IR spectral energy distribution (SED) that shows a large excess with a maximum at 10–30 μm and a strong decrement beyond these wavelengths.

A star location outside a region of star formation.



FS CMa group

It has 70 members between confirmed and candidate ones (Kuratova et al. 2019).

They are suspected to be binaries at a post-mass-exchange evolutionary phase, with a secondary component fainter and cooler than the primary or degenerate (Miroshnichenko, 2007, Miroshnichenko et al. 2007, 2009).

However, only 15 objects of this class have been confirmed as binary systems and 6 as candidates (Miroshnichenko et al. 2023).

Table 2. Detected or suspected FSCMa-type binary systems.

Star ID	V	Sp.T.	Period
MWC 623	10.8	B4 v + K2 III	—
CI Cam	11.6	B2 III + ?	19.41 ± 0.02
V669 Cep	12.2	B4/6 + lt	—
HD 50138	6.6	B5/6 v	—
FS CMa	7.0–8.9	B2 v	—
HD 85567	8.6	B5 v	—
IRAS 07377–2523	12.8	B8/A0 + lt	—
FX Vel	9.4–11.4	A + lt	—
AS 174	11.5	A + lt	—
IRAS00470 + 6429	12.0	B2 v + lt?	—
MWC 728	9.8	B5 v + G8 III	27.50 ± 0.11
AS 386	10.9	B9 Ib + ?	131.27 ± 0.09
3 Pup	4.0	A3 Ib + sd O	137.4 ± 0.1
MWC 645	12.8–13.4	B2 v + K2 III	—
HD 327083	9.7–10.1	B1 I + F1 I	107.68 ± 0.02

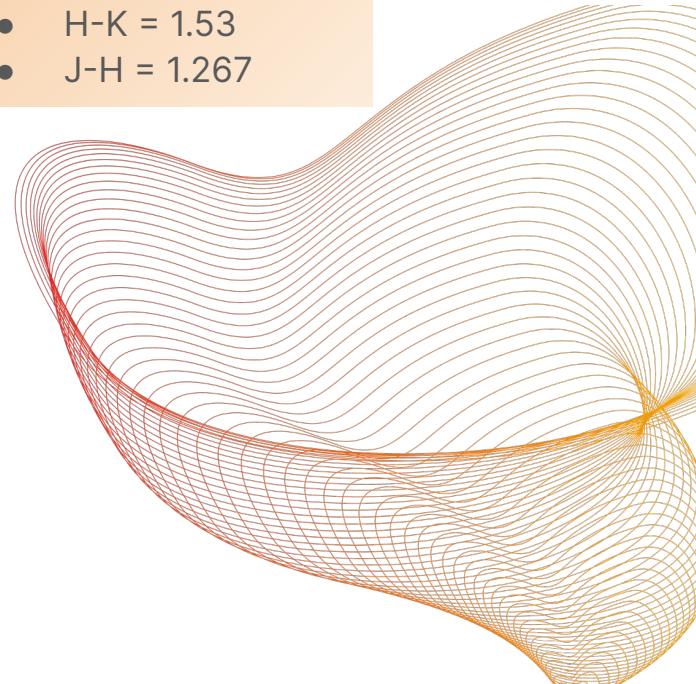


MWC 645 = V 2211 Cyg



- $\alpha = 21:53:27.49$
- $\delta = +52:59:58.01$

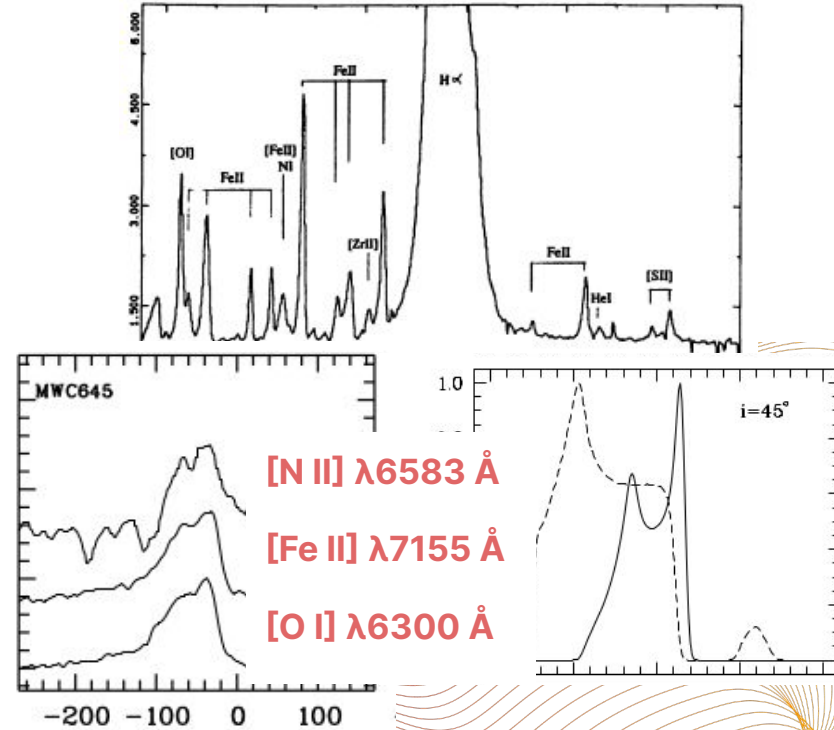
- $V = 13.0$
- $H-K = 1.53$
- $J-H = 1.267$





MWC 645: Background

- Strong emission lines of H I, Fe II and [Fe II]; striking similarities with Eta Car (Merrill & Burwell 1943; Swings & Allen 1973).
- Photometric variability: amplitude ~ 0.3 mag, period ~ 23.6 yrs (Gottlieb & Liller 1978).
- No stellar absorption features.
- Possible detection of He I lines (late B-type star).
- Detection of lines typically seen in spectral types later than F (Jaschek et al. 1996).
- Member of the UnclB[e] stars group (Lamers et al. 1998).
- Asymmetric emission line-profiles for metallic lines.
- Split emission lines of [O I] and [Fe II].
- A peculiar emission profile of the H α line: a broad blue and a narrow red components, with FWHM ~ 5.0 Å and 1.3 Å, respectively (Zickgraf 2003).



To explain the observations:

Zickgraf proposed a latitude-dependent wind model with a large optical depth dust disk at an intermediate inclination.



MWC 645: Background

Nodyarov et al. (2022) found:

- Absorption lines of neutral metals (Li I, Ca I, Fe I, Ti I, V I, and Ni I) with radial velocity variations revealing the binary nature of the object.
- No absorption line typical of a B-type object.
- Near-IR emission lines of H I, Fe II, O I, N I, and He I.
- Photometric quasi-cyclic variations (with periods of months and ~ 4 years).
- Two weak emission peaks at $\sim 10 \mu\text{m}$ and $18 \mu\text{m}$ in the SED (presence of silicates).
- For the hot component: $T_{\text{eff}} = 18,000 \pm 2000 \text{ K}$, $\log(L/L_{\odot}) = 4.0 \pm 0.5$.
- For the cool component: $T_{\text{eff}} = 4250 \pm 250 \text{ K}$, $\log(L/L_{\odot}) = 3.1 \pm 0.3$.

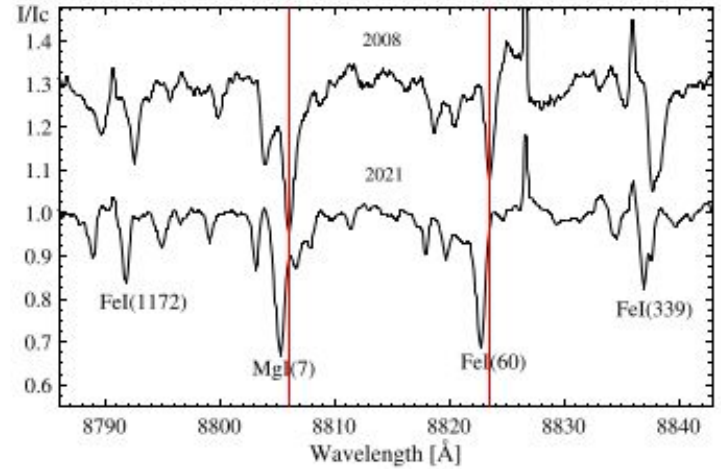


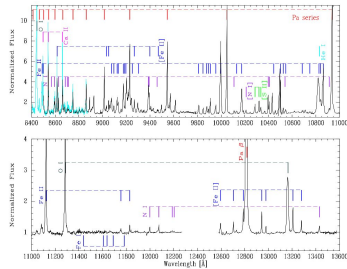
Figure 4. Comparison of a part of the spectra with absorption lines taken in 2008 and 2021 CFHT. Vertical lines show positions of some lines in the 2008 spectrum, to outline the shift from those in the 2021 spectrum.

They concluded that:

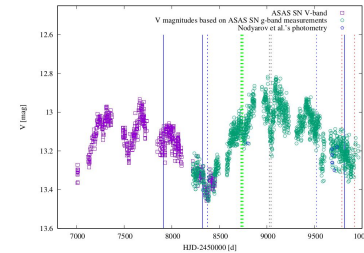
The star can be classified as an **FS CMa**-type object, where its intermediate-mass components ($7 M_{\odot}$ and $2.8 M_{\odot}$) undergo an ongoing mass-transfer process.

Our study on MWC 645

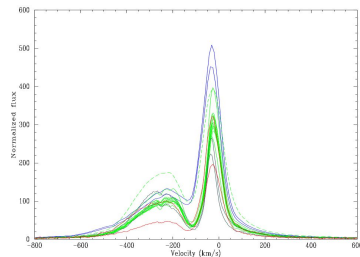
01 Near-IR Spectra: K- and L- bands



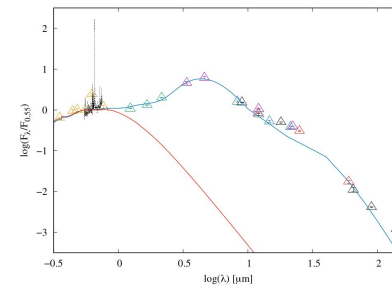
02 Optical Photometric Light Curve



03 Optical Spectra: H α line spectral region



04 Spectral Energy Distribution





Observations

Gemini North Observatory, Hawaii:

Near-IR spectra taken with the Gemini Near-Infrared Spectrograph (GNIRS).

Observations Program ID	Spectral Range [Å]
GN-2017A-Q-62	22,570-24,400
GN-2018A-Q-406	21,000-24,500
GN-2018A-Q-406	15,800-18,200
GN-2018A-Q-406	11,000-13,600
GN-2018A-Q-406	8400-11,000
GN-2022B-Q-225	33,311-36,446
GN-2022B-Q-225	38,500-41,786

- K-band spectra: (R~5500)

Instrumental configuration: a 110.5 l/mm grating, a 0.3 arcsec slit, and the short camera (0.15 arcsec/pix).

Long-slit mode centered at 2.35 μm (Program ID: GN-2017A-Q-62).

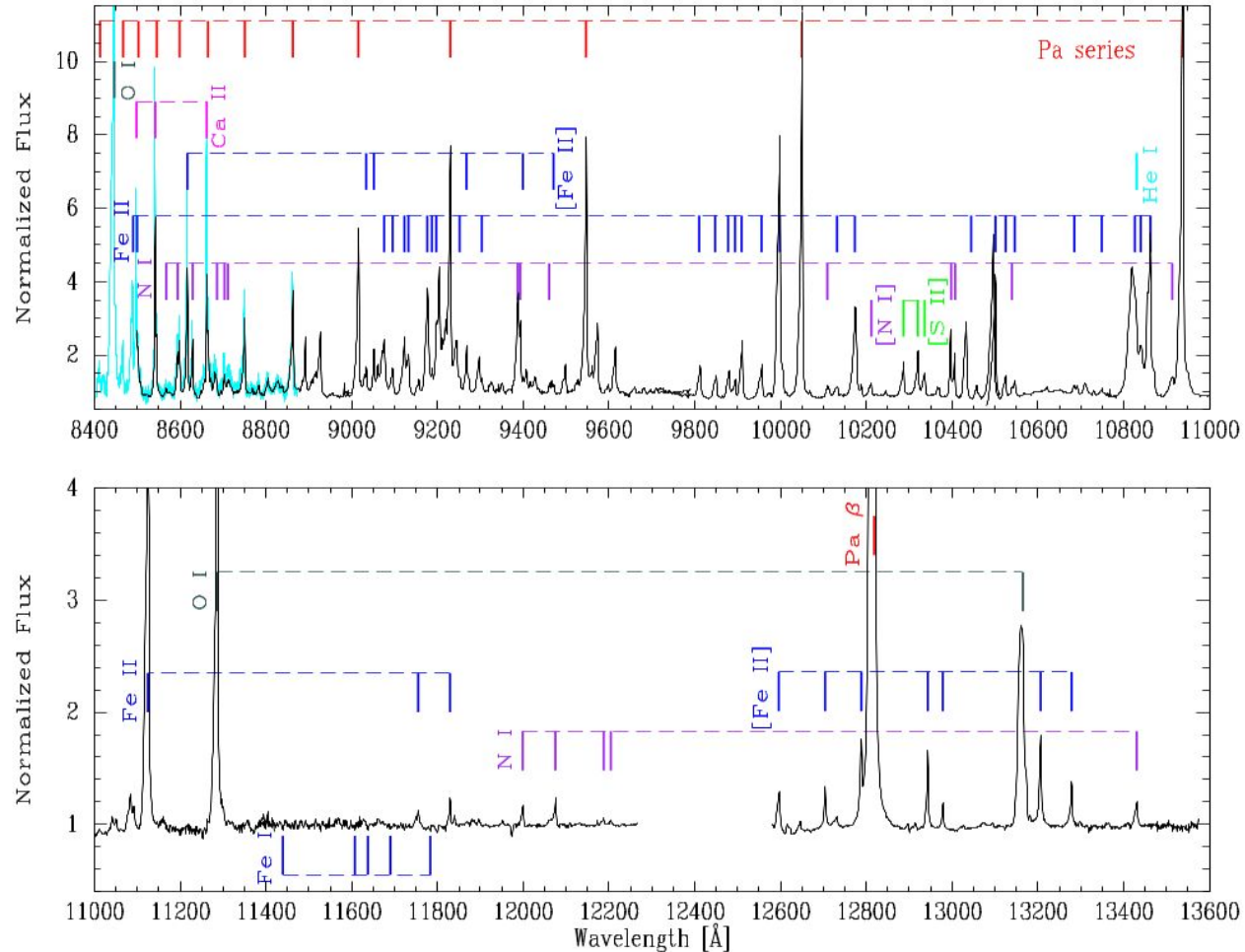
Cross-dispersed mode centered at 2.19 μm and 2.36 μm (Program ID: GN-2018A-Q-406).

- L-band spectra: (R~5100)

Long-slit configuration: a 31.7 l/mm grating, a 0.1 arcsec slit, and the long camera (0.05 arcsec/pix), centered at 3.48 and 4.00 μm (Program ID: GN-2022B-Q-225).

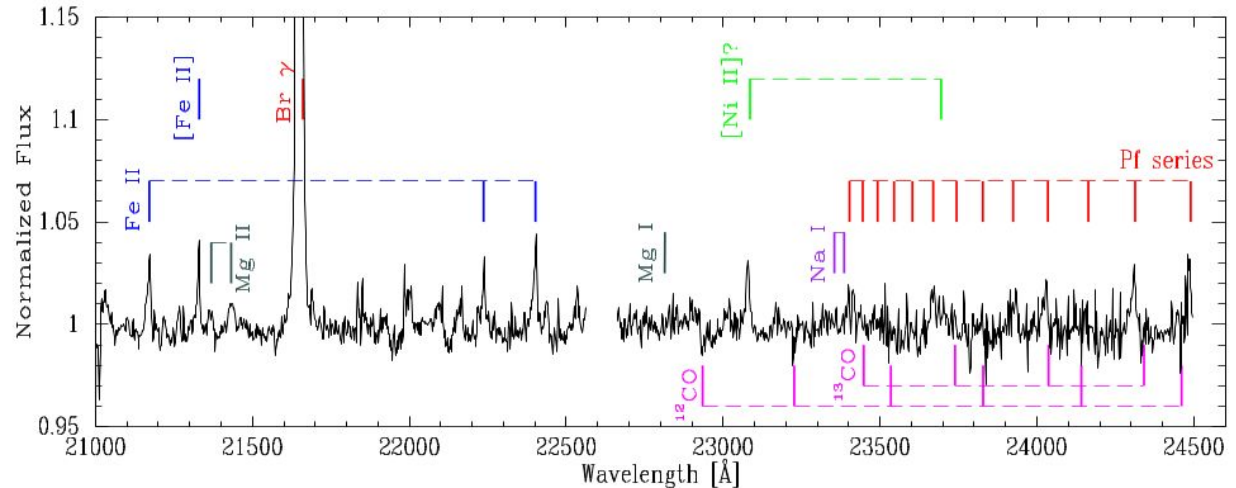
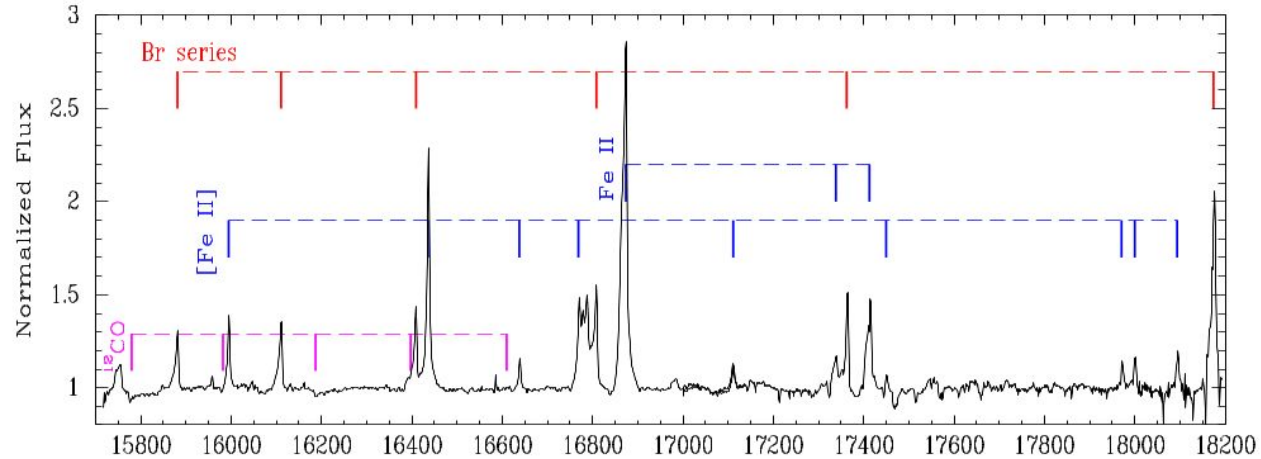
Near-IR Data

- The strongest lines are the H I Paschen series, O I, Fe II, and Ca II triplet lines.
- Transitions of N I, [Fe II] and [S II] are present.
- Absorption lines of Fe I were identified.
- If He I lines are present, they are incipient and hidden in the noise.



Near-IR Data

- The H I Brackett series and several permitted and forbidden lines of Fe II are the dominant transitions.
- The most intense feature is the Br γ line.
- Mg II $\lambda\lambda$ 21,374 Å and 21,437 Å lines and the Pfund series are in emission.
- Absorption features of neutral metals (Ca I, Mg I, and Na I) are identified.
- For the first time, we have detected the CO band heads in absorption at $\sim 2.3 \mu\text{m}$ and $\sim 1.6 \mu\text{m}$.





Observations

Gemini North Observatory, Hawaii:

Near-IR spectra taken with the Gemini Near-Infrared Spectrograph (GNIRS).

Observations Program ID	Spectral Range [Å]
GN-2017A-Q-62	22,570-24,400
GN-2018A-Q-406	21,000-24,500
GN-2018A-Q-406	15,800-18,200
GN-2018A-Q-406	11,000-13,600
GN-2018A-Q-406	8400-11,000
GN-2022B-Q-225	33,311-36,446
GN-2022B-Q-225	38,500-41,786

- K-band spectra: (R~5500)

Instrumental configuration: a 110.5 l/mm grating, a 0.3 arcsec slit, and the short camera (0.15 arcsec/pix).

Long-slit mode centered at 2.35 μm (Program ID: GN-2017A-Q-62).

Cross-dispersed mode centered at 2.19 μm and 2.36 μm (Program ID: GN-2018A-Q-406).

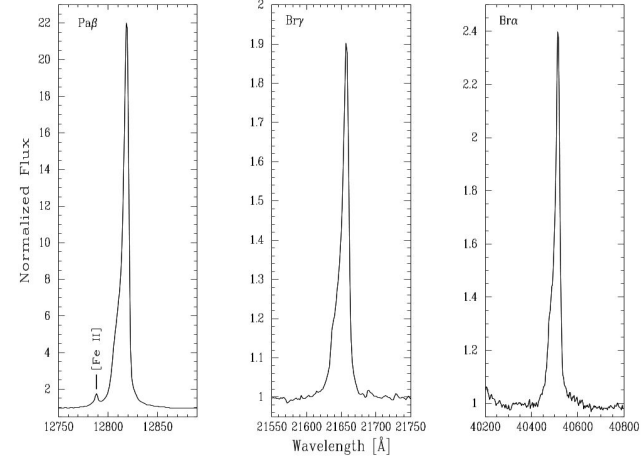
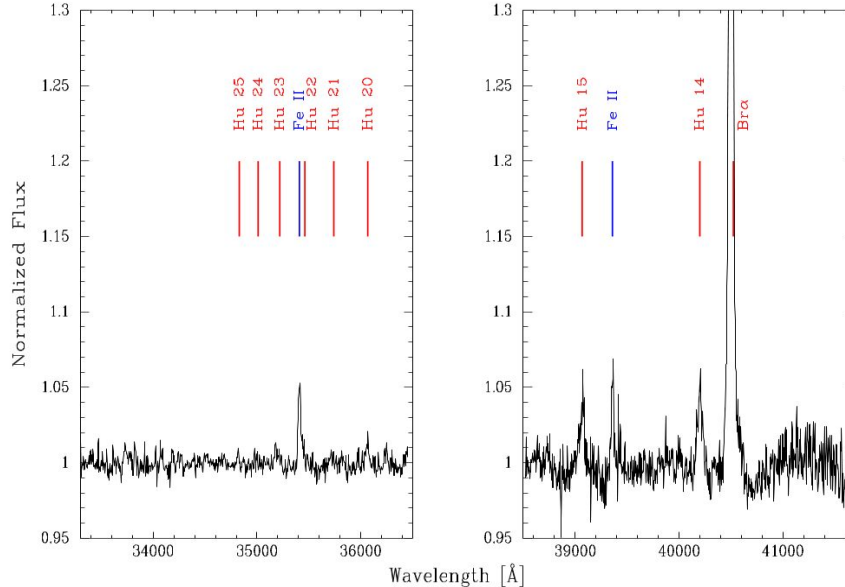
- L-band spectra: (R~5100)

Long-slit configuration: a 31.7 l/mm grating, a 0.1 arcsec slit, and the long camera (0.05 arcsec/pix), centered at 3.48 and 4.00 μm (Program ID: GN-2022B-Q-225).



Near-IR Data

- Left: Fe II λ 35,423 Å line and H I lines of the Humphreys series are in emission.
- Right: Humphreys series members and Br α line can be seen.



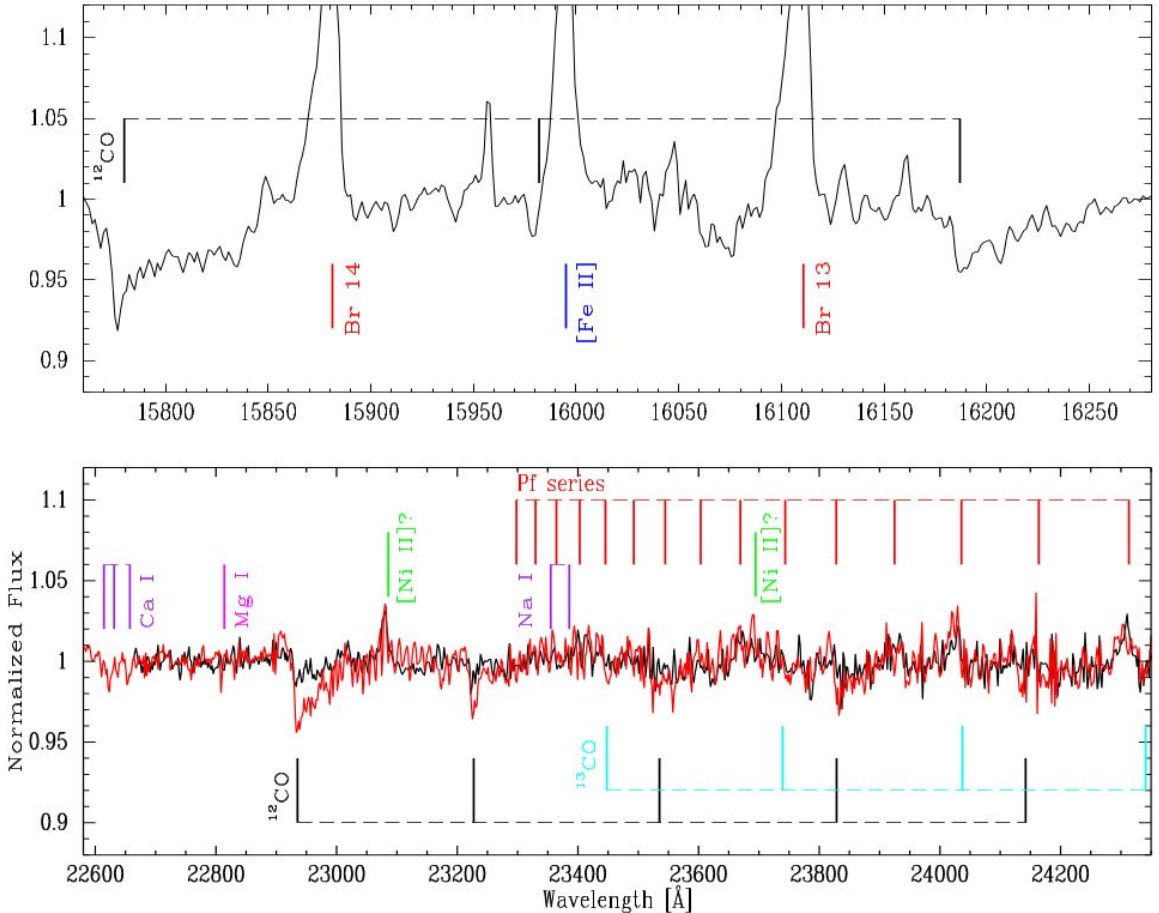
- Pa β , Br γ , and Br α lines have single-peaked and asymmetric profiles.

- We found no absorption bands of the first-overtone of SiO at $\sim 4 \mu\text{m}$.



CO Band heads

- Top: Second-overtone band heads of 12 CO in absorption from the 2018 spectrum.
- Bottom: Comparison between the K-band spectrum taken in 2017 (red) and in 2018 (black), where the variation of the first-overtone band heads of 12 CO is seen.
- The positions of the 13 CO band heads are detected in the spectrum from 2017.





CO Band heads

The strength of the CO absorption bands of classical late-type stars depends on the T_{eff} and $\log g$ (Kleinmann & Hall, 1986; Mármol-Queraltó et al. 2008).

- To characterize the cool companion of MWC 645, we compare our spectrum from 2017 with:
 - Spectra from the IRTF Spectral Library ($R \sim 2000$).
 - For stars with spectral types F - M and luminosity classes I - V.

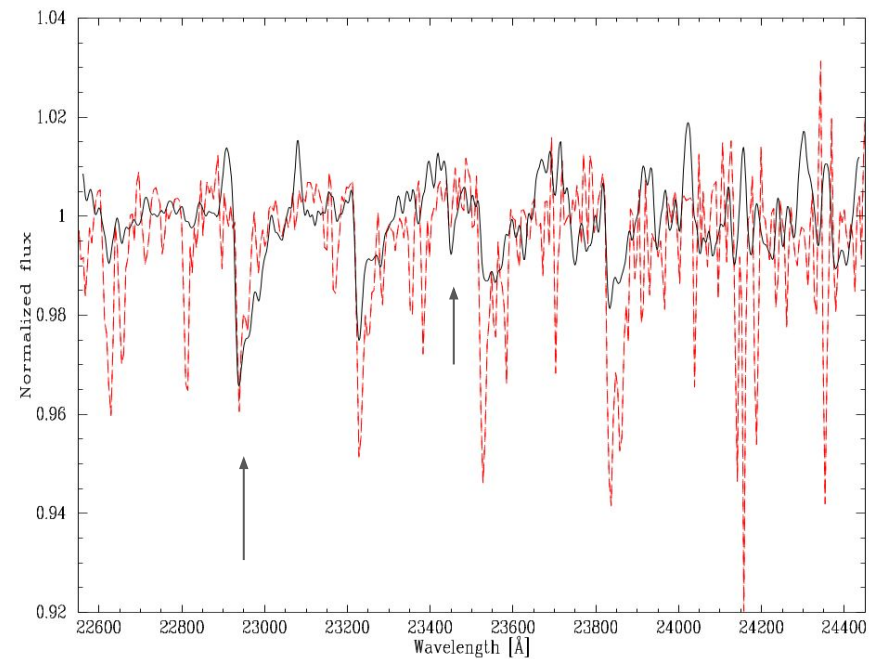


Figure: The MWC 645 spectrum (black line) compared to a G0 Ib-II star (HD 185018) spectrum (red line).

The intensity of the first 12 CO band head of MWC 645 coincides well, but not the the rest of them.

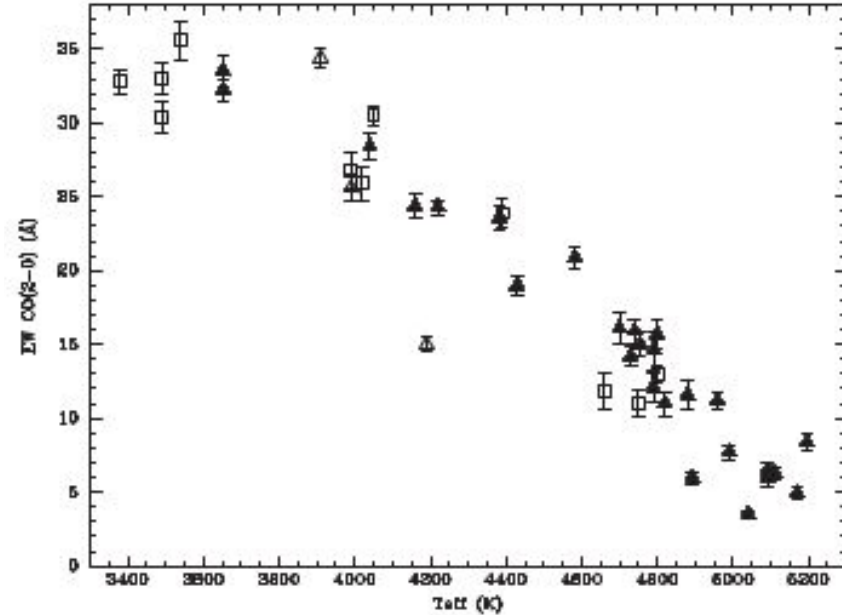
The absorption of the 13 CO band head is more intense than that displayed by the library star.

The absorption lines of neutral metals weaker than those in the template spectrum and the lack of SiO band heads at $4 \mu\text{m}$, indicate an earlier spectral type.



12 CO Band heads

- Winge et al. (2009) presented a spectroscopic library of late spectral-type stellar templates in the K-band at $R \sim 5900$.
- They plotted $EW\ CO(2,0)$ vs. T_{eff} for a stellar sample with T_{eff} in the range 3200–5200 K and different luminosity classes



We measured from the spectrum of:

- 2017: $EW\ CO(2,0) = 2.55 \pm 0.5 \text{ \AA}$
 - $T_{eff} \sim 5200 \pm 100 \text{ K}$
- 2018: $EW\ CO(2,0) = 1.22 \pm 0.1 \text{ \AA}$
 - $T_{eff} \sim 5300 \pm 100 \text{ K}$.

Winge et al. (2009).



Observations

Ondřejov Observatory, Czech Republic:

Optical spectra taken in September 2018 with the Coudé spectrograph ($R \sim 12,000$).

Instrumental configuration: a grating of 830.77 l/mm, a SiTe 2030 × 800 CCD and a slit width of 0.7 arcsec.

Wavelength coverage: 6262 - 6735 Å and 8400 - 8860 Å.

Tartu Observatory, Estonia:

Low resolution optical spectrum taken in November 2021 with the long-slit spectrograph ASP-32 with a grating of 600 l/mm.

Wavelength coverage: 5450 - 7480 Å.

BeSS database:

Spectra taken between 2019 and 2022 with 1) $R \sim 14,000/16,000$ and 2) $R \sim 5000$.

Wavelength coverage: 1) 6500 - 6600 Å and 2) 6150 - 7000 Å.

ASAS-SN survey:

Photometric data obtained over eight years. V-band magnitudes from December 2014 to November 2018, 2) g-band magnitudes from April 2018 to January 2023.

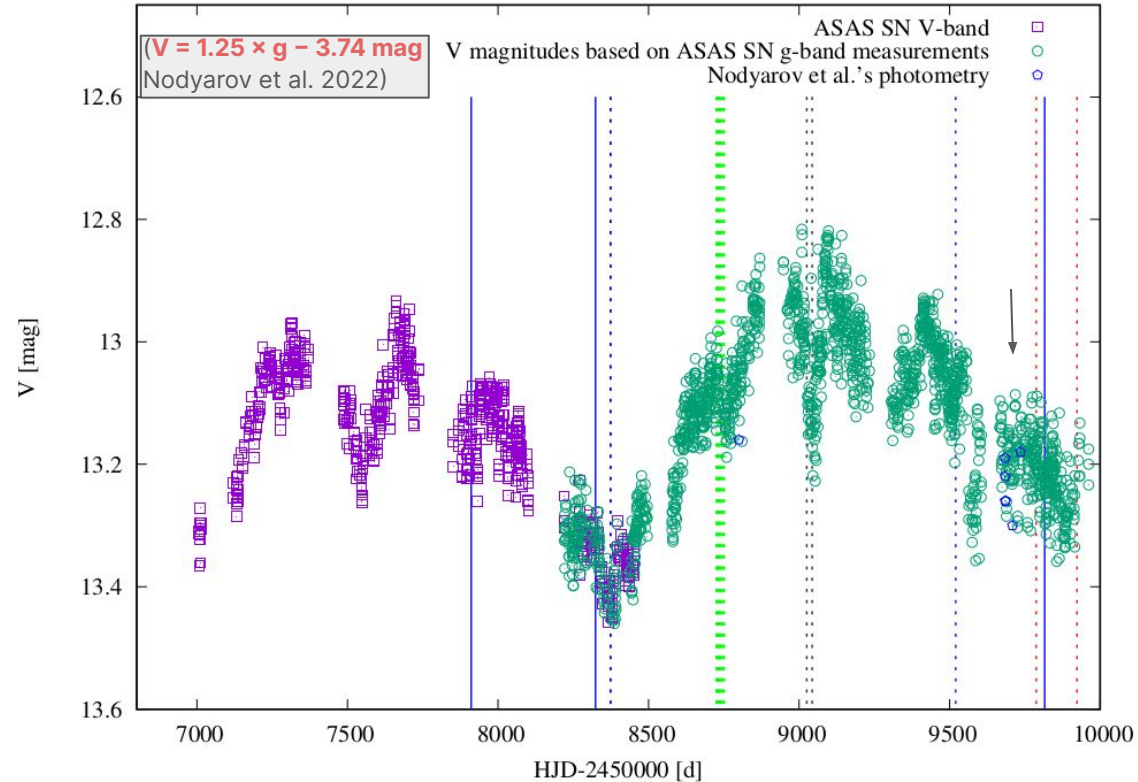
Vizier service:

Ground- and space-based multicolor photometry from 0.3 μm to 140 μm.



Optical Photometric Light Curve (LC)

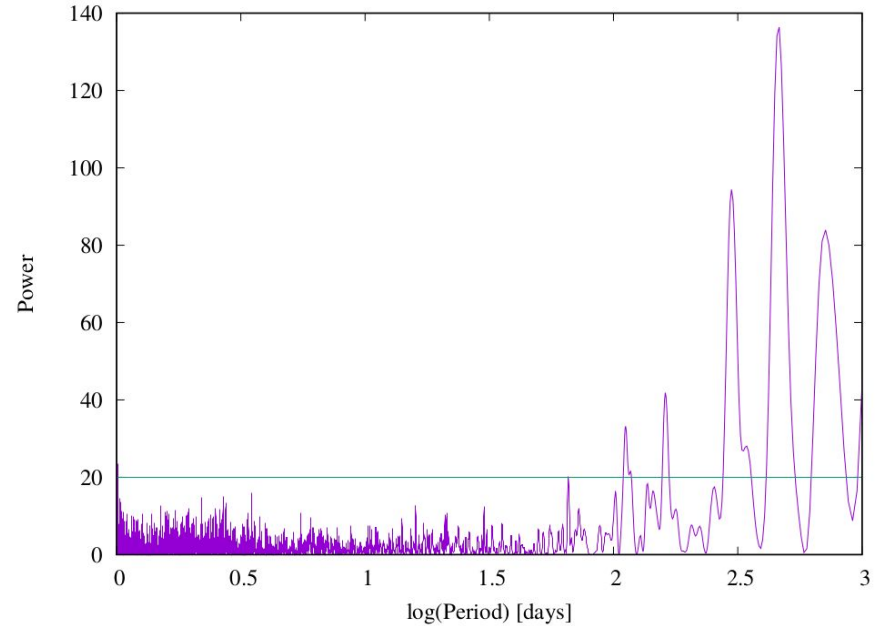
- Nodyarov et al. (2022) suggested that a new minimum might take place in the second half of 2022.
- The star continued fading up to the end of October and then, it began to strengthen in brightness again.
- We applied the Lomb–Scargle method using the IRSA time series tool to the V-band LC.
- We discarded the magnitudes with errors greater than 0.03 mag.





Periodogram

- The scan of periodic signals with values below ten days gave strong peaks at one day and harmonics of the sidereal day.
- The periodogram for periods greater than one day is shown in the Figure.
- The periodogram (for $P > 1$ d) gives six peaks at or above a confidence level of 20 in the power spectrum for $P \sim$ 65, 112, 162, 298, 461, and 709 d.
- The phase diagram for each period shows a large scatter of the magnitude points and a small amplitude in their modulation (~ 0.2 – 0.3 mag).
- We recovered two periods found by Nodyarov et al. (2022).





Observations

Ondřejov Observatory, Czech Republic:

Optical spectra taken in September 2018 with the Coudé spectrograph ($R \sim 12,000$).

Instrumental configuration: a grating of 830.77 l/mm, a SiTe 2030 \times 800 CCD and a slit width of 0.7 arcsec.

Wavelength coverage: 6262 - 6735 Å and 8400 - 8860 Å.

Tartu Observatory, Estonia:

Low resolution optical spectrum taken in November 2021 with the long-slit spectrograph ASP-32 with a grating of 600 l/mm.

Wavelength coverage: 5450 - 7480 Å.

BeSS database:

Spectra taken between 2019 and 2022 with 1) $R \sim 14,000/16,000$ and 2) $R \sim 5000$.

Wavelength coverage: 1) 6500 - 6600 Å and 2) 6150 - 7000 Å.

ASAS-SN survey:

Photometric data obtained over eight years. V-band magnitudes from December 2014 to November 2018, 2) g-band magnitudes from April 2018 to January 2023.

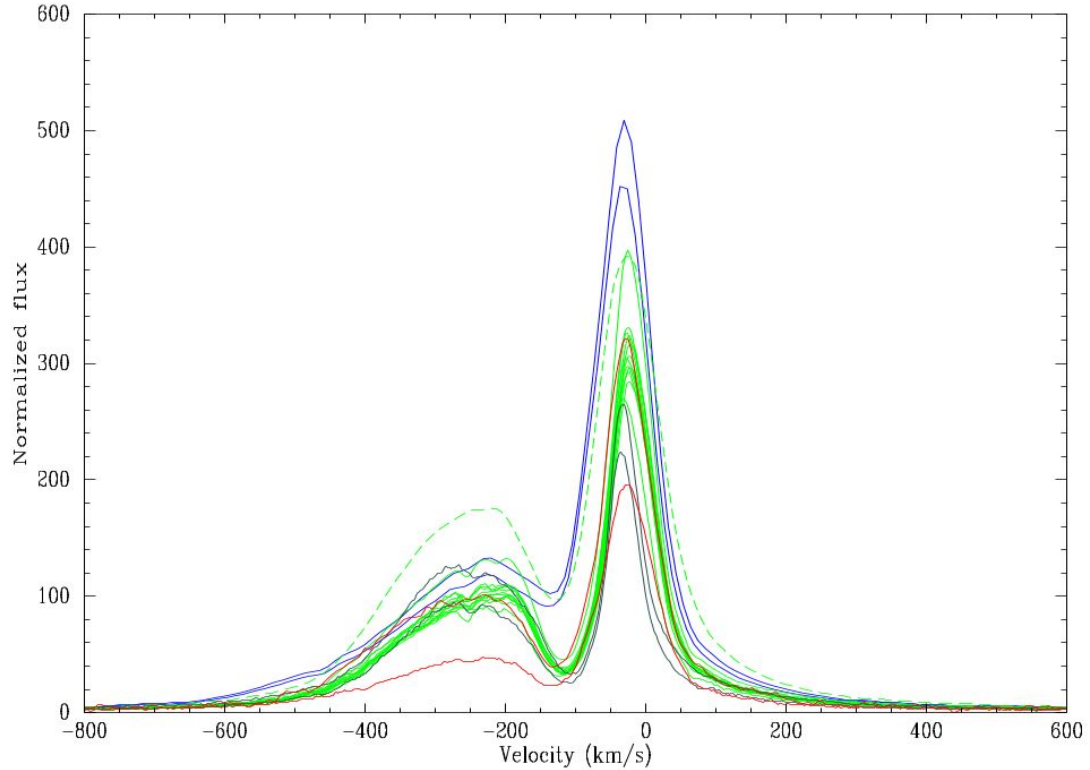
Vizier service:

Ground- and space-based multicolor photometry from 0.3 μm to 140 μm .



H α Line-profile

- Spectra taken in 2018 (from Ondrejov), 2019, 2020, and 2022 (from BeSS database) are displayed in blue, green, gray, and red, respectively.
- BeSS spectra are not corrected by telluric lines.
- The profile of the H α line is composed of a broad blue-shifted peak and a narrow red-shifted one.
- A variation in the emission strength of both peaks is seen.





H α Line-profile

- The V/R ratio presents changes over 4 years, even doubling its value.
- The ratio of V/R \sim 0.3 corresponds to observations close in time, where, the changes in EW might be mainly due to the continuum-level variations.

Obs. Date (yyyy-mm-dd)	HJD-2450000	Observatory	V	R	V/R	EW [Å]
2018-09-11	8373.3290	Ondřejov	118.4	452.0	0.26	-1980.3
2018-09-12	8374.2823	Ondřejov	132.8	509.0	0.26	-2122.8
2019-08-28	8724.3870	BeSS ¹	90.2	268.9	0.33	-1132.2
2019-08-30	8726.4279	BeSS ²	75.1	391.9	0.45	-2130.7
2019-09-01	8728.4429	BeSS	95.7	283.9	0.34	-1237.2
2019-09-02	8729.4419	BeSS	105.7	316.0	0.33	-1291.7
2019-09-03	8730.4365	BeSS	101.5	306.1	0.33	-1353.7
2019-09-05	8732.4433	BeSS	100.1	292.3	0.34	-1147.3
2019-09-07	8734.3942	BeSS	109.7	323.5	0.34	-1372.1
2019-09-10	8737.3883	BeSS	99.8	296.0	0.34	-1292.5
2019-09-11	8738.3925	BeSS	132.3	397.1	0.33	-1642.3
2019-09-14	8741.4241	BeSS	110.5	330.9	0.33	-1348.1
2019-09-19	8746.3989	BeSS	100.5	297.7	0.34	-1129.5
2019-09-20	8747.3862	BeSS	103.1	304.3	0.34	-1264.6
2019-09-24	8751.3722	BeSS	109.1	326.1	0.33	-1283.5
2020-06-25	9025.5535	BeSS	94.1	223.7	0.42	-933.8
2020-07-12	9043.5126	BeSS	127.4	264.8	0.48	-1216.8
2021-11-01	9520.3161	Tartu	—	—	—	—
2022-07-26	9787.5322	BeSS	47.3	195.6	0.24	-718.2
2022-12-09	9923.2775	BeSS	100.5	321.2	0.31	-1392.3

¹ For details about the instruments and observers, please visit the web page BeSS database (<http://basebe.obspm.fr/basebe/>) (accessed on 2 February 2023). ² Spectrum with the lowest resolution.



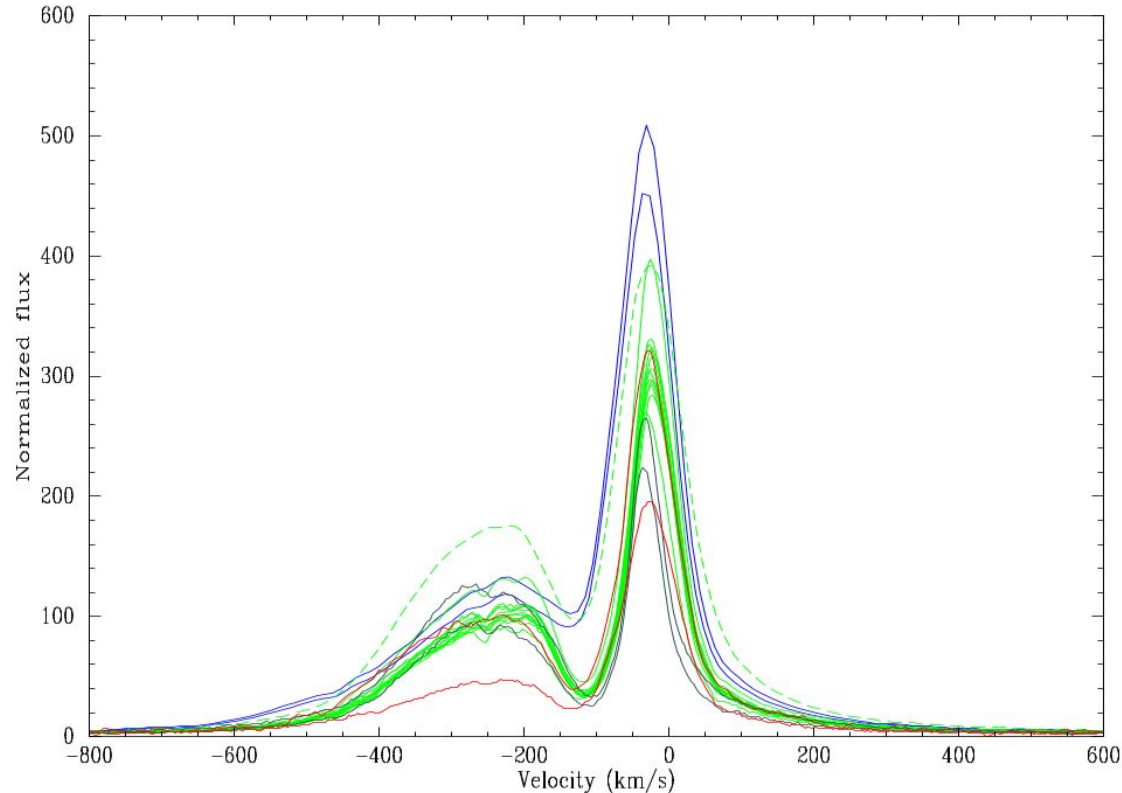
H α Line-profile

From the Ondrejov spectra we derived for the blue and red emission components:

- an average radial velocity of -225 ± 5 km/s and -31 ± 3 km/s, respectively, in agreement with the values reported by Zickgraf (2003) and Nodyarov et al. (2022)
- an average FWHM of 318 ± 4 km/s and 90 ± 1 km/s, respectively.

And from the BeSS spectra:

- an average radial velocity of -229 km/s and -26 km/s, respectively
- an average FWHMs of 256 ± 4 km/s and 80 ± 2 km/s, respectively.



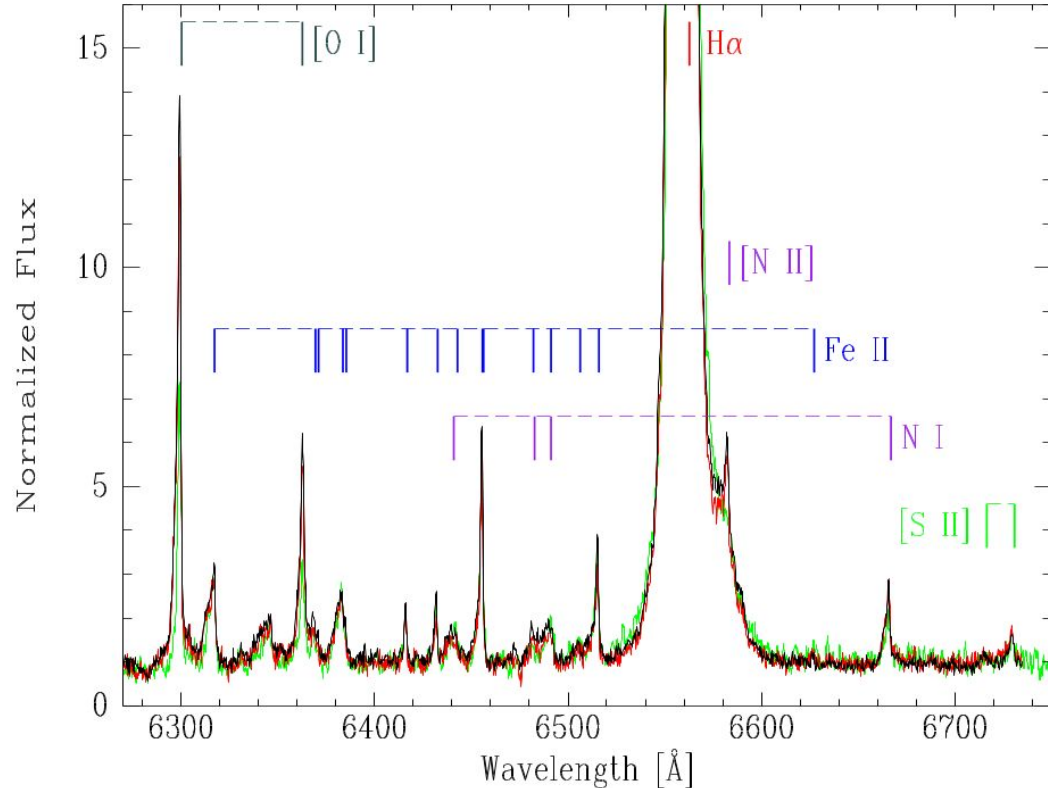


H α Line spectral region

- [O I] $\lambda\lambda$ 6300, 6364 Å lines appear single-peaked, although asymmetric.
- Several permitted Fe II lines and the forbidden lines of [N II] λ 6583 Å and [S II] $\lambda\lambda$ 6716, 6731 Å are apparent.
- The He I λ 6678 Å transition is absent.

We derived an average heliocentric radial velocity of the emission lines of the Ondřejov spectra, obtaining -43 ± 2 km/s.

Jaschek et al. (1996) and Nodyarov et al. (2022) obtained -76 ± 5 km/s and -61 ± 4.3 km/s, respectively, indicating variability.





Observations

Ondřejov Observatory, Czech Republic:

Optical spectra taken in September 2018 with the Coudé spectrograph ($R \sim 12,000$).

Instrumental configuration: a grating of 830.77 l/mm, a SiTe 2030 \times 800 CCD and a slit width of 0.7 arcsec.

Wavelength coverage: 6262 - 6735 Å and 8400 - 8860 Å.

Tartu Observatory, Estonia:

Low resolution optical spectrum taken in November 2021 with the long-slit spectrograph ASP-32 with a grating of 600 l/mm.

Wavelength coverage: 5450 - 7480 Å.

BeSS database:

Spectra taken between 2019 and 2022 with 1) $R \sim 14,000/16,000$ and 2) $R \sim 5000$.

Wavelength coverage: 1) 6500 - 6600 Å and 2) 6150 - 7000 Å.

ASAS-SN survey:

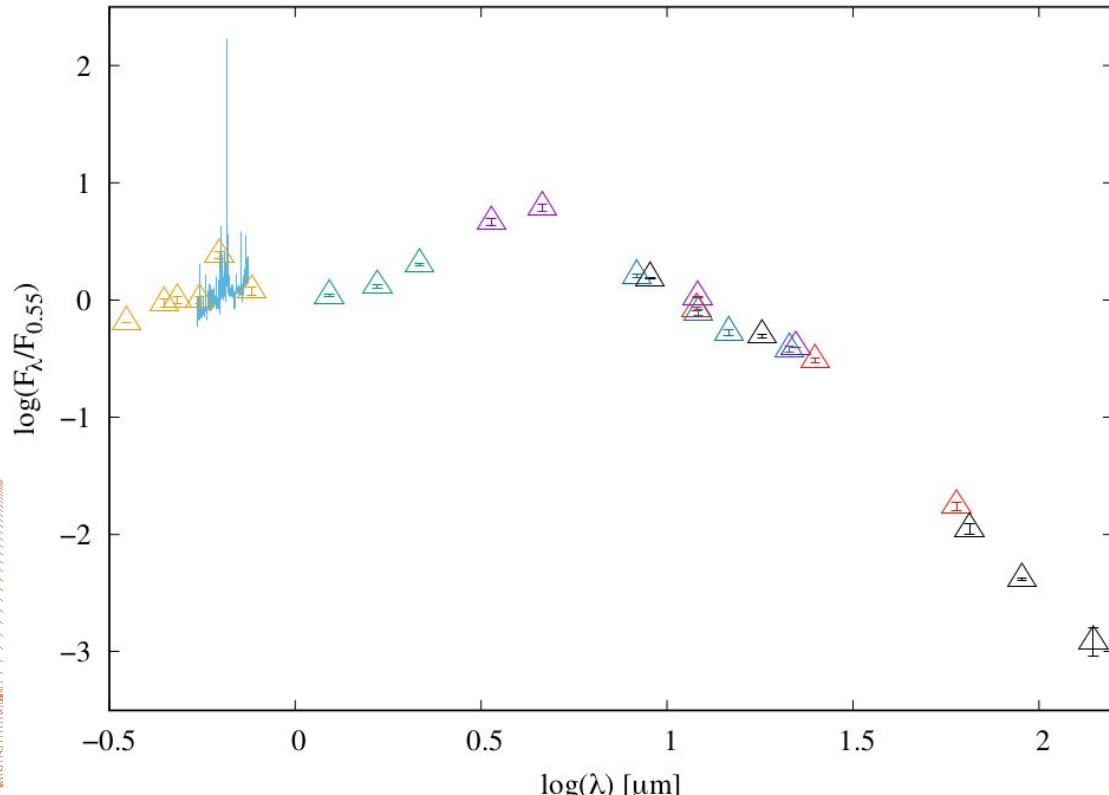
Photometric data obtained over eight years. V-band magnitudes from December 2014 to November 2018, 2) g-band magnitudes from April 2018 to January 2023.

Vizier service:

Ground- and space-based multicolor photometry from 0.3 μm to 140 μm .



Observed SED



SED of MWC 645 built from the photometry publicly available from 0.3 μm –140 μm .

Optical bands in yellow, 2MASS in green, WISE in violet, MSX in light blue, IRAS in red, and AKARI in black.

The low-resolution spectrum acquired in 2021 over the H α region is also displayed (light blue line).



Global Properties of the CS Material

To derive the global physical properties of the CS material, we considered the SED is assembled by different envelope components (Marchiano et al., 2013, Arias et al. 2018).

The model: a spherical envelope composed of gas close to the star ($\leq 5 R_*$) and (or) dust further away from it ($\geq 100 R_*$).

The emergent flux is computed from the central star and the envelope, applying a plane-parallel solution for the transfer equation.

The gaseous shell is characterized by $\tau^G(\lambda)$ and $S^G(\lambda)$ with T^G and R^G as free parameters.

The dusty region is described by $\tau^D(\lambda)$, T^D and R^D , where:

$$T^D(r) = T_{\text{eff}} W(r)^{[1/(4+p)]}, p \sim 1.$$

The model allows several dust shell components to be added.

The interstellar extinction is also included by $\tau^{\text{ISM}}(\lambda)$.

The absorption $A(\lambda)$ is related to each optical depth through $\tau = 0.4 \ln(10) A(\lambda)$.

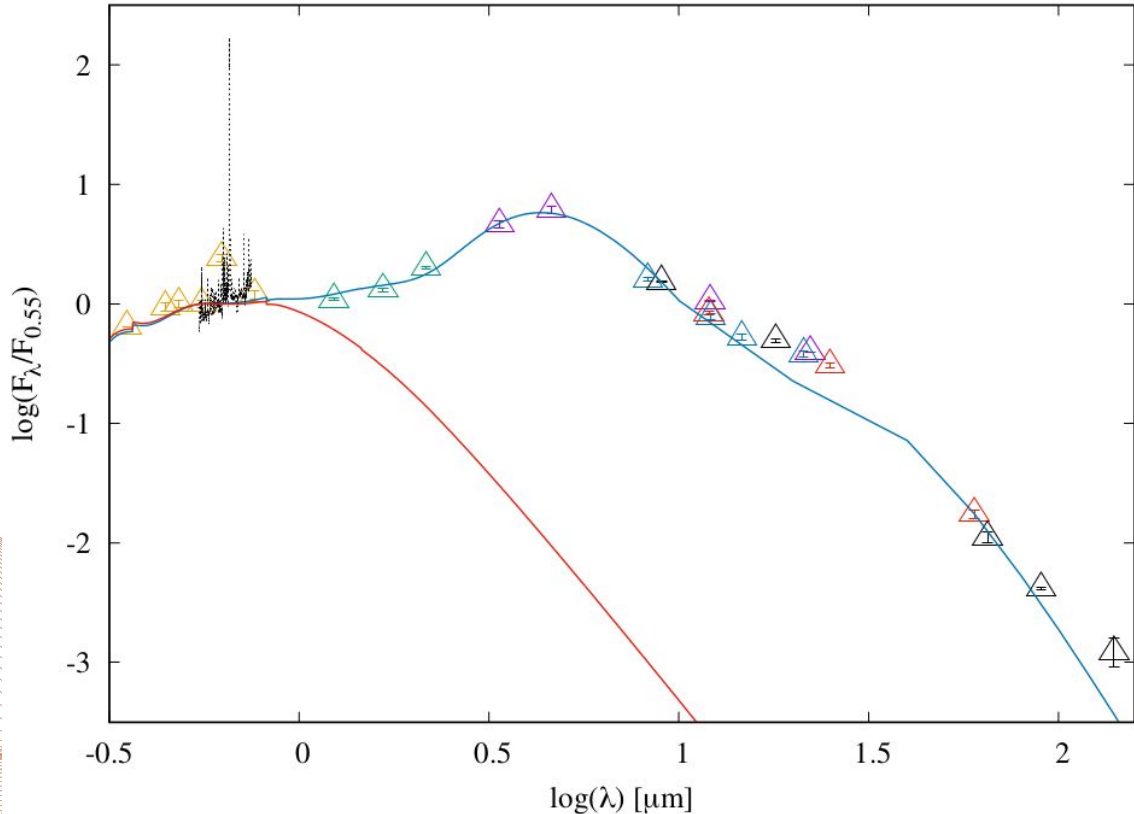
Using the law given by Cardelli et al. (1989):

$$A(\lambda) = [R_V a(1/\lambda) + b(1/\lambda)] E(B-V),$$

where R_V is the total to selective extinction and $E(B-V)$ is the colour excess.



Global Properties of the Circumstellar (CS) Material

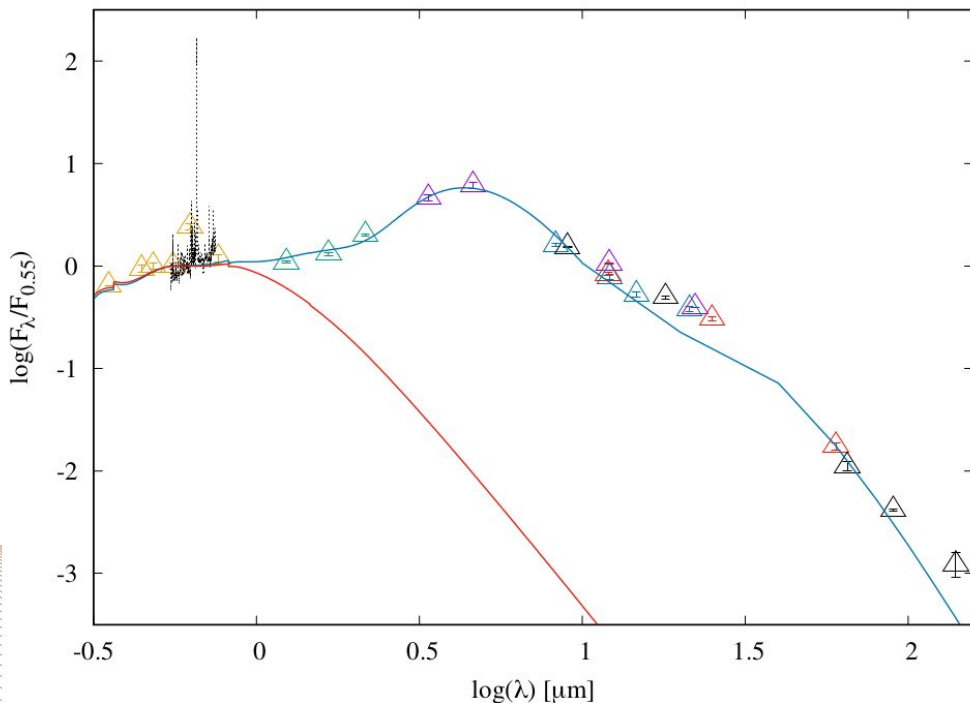


Solid red line: modeled SED considering the contribution of the **photospheric fluxes from both stars**, the **thermal emission from a gaseous shell** close to the system and the **effect of the interstellar medium extinction**.

Solid blue line: best-fitting theoretical SED, obtained by **adding** to the SED plotted in red the contribution of **three dusty shells** surrounding the stellar system.



Global Properties of the Circumstellar (CS) Material



The disagreement between the theoretical and observed SEDs in the region of 10 μm to 18 μm might be due to the presence of silicate particles.

Best-fitting model:

- 80% from a star with $T_{\text{eff}} = 18,000 \text{ K}$, $\log g = 4.0$, and $R^* = 3.73 R_{\odot}$
- 20% from a cool star with $T_{\text{eff}} = 5000 \text{ K}$ and $\log g = 1.5$.

Resulting envelope:

- a gaseous shell: $R^G = 1.15 R^*$, $T^G = 16780 \text{ K}$ and $\tau_V = 0.1$.
- three dusty shells:
 - $R_1^D = 348 R^*$, $T_1^D = 1310 \text{ K}$
 - $R_2^D = 3750 R^*$, $T_2^D = 507 \text{ K}$
 - $R_3^D = 0.02 \text{ pc}$, $T_3^D = 98 \text{ K}$.
 -

Total visual absorption: $A_V = 3.13 \pm 0.11 \text{ mag}$ (in agreement with Nodyarov et al. (2022)).



Results and Possible Scenarios...

1) Presence of CS Gas and

Dust: The IR spectral analysis reveals their presence and poses challenges in characterizing the binary system and in the construction of possible scenarios.

2) Hot Component Classification:

It was considered an early-B type star, by the absence of He II lines and possible presence of He I absorption lines in the optical range (Nodyarov et al 2022).

We did not detect He I lines in the IR, but a blend of He I at $1.083 \mu\text{m}$ with Fe II emission lines might exist.

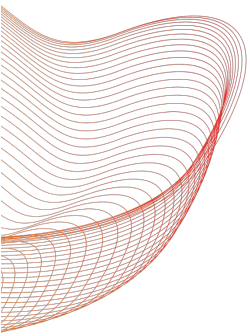
According to Clark and Steele's works (2000, 2001) in the IR, emission from Mg II and Bry lines point toward a spectral type between B2 and B4, or B3 (or earlier) if He I lines are present.

3) CO Absorption Bands and Cool Component Spectral

Type: Newly detected ^{12}CO absorption bands at $1.62 \mu\text{m}$ and $2.3 \mu\text{m}$ helped determine the cool binary component's spectral type and T_{eff} .

The G0-type star fit contradicts weak metallic lines observed in MWC 645's spectra.

Due to the contribution of the hot companion and ionized envelope in the near-IR spectrum, the T_{eff} , estimated from the CO(2,0) band head EW, serves as an upper limit.



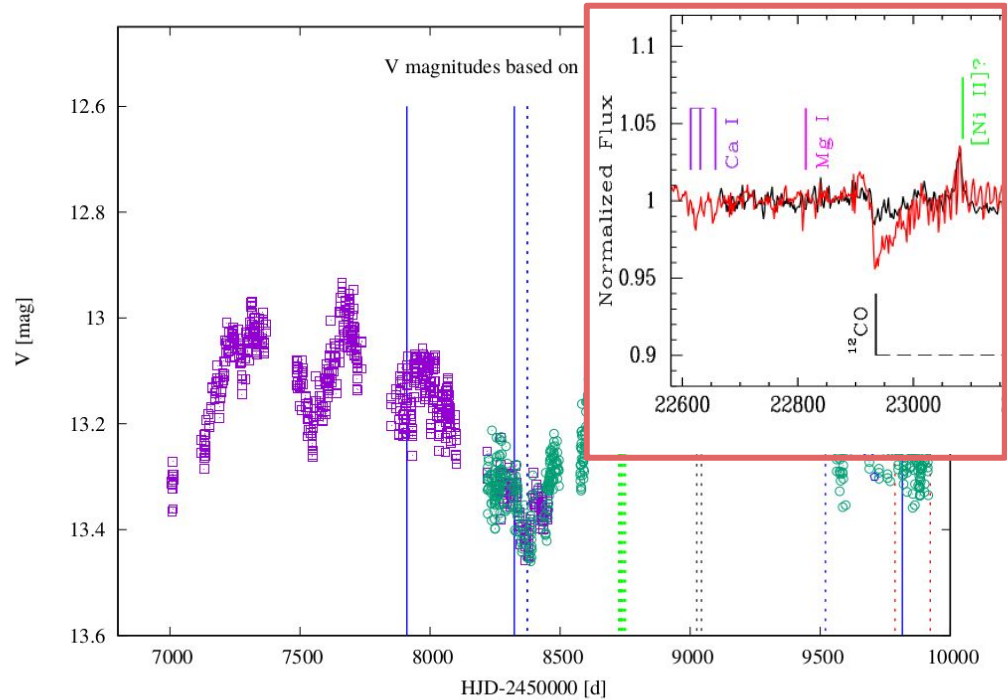
Results and Possible Scenarios...

4) CO Absorption and Mass Ejection:

The CO absorption bands might indicate a mass-ejection episode, where molecular absorption bands develop as star brightness fades, as in the case of ρ Cas (Gorlova et al. 2006, Kraus et al. 2019) and V838 (Geballe et al. 2007).

A strong CO absorption in 2017 coincides with increased brightness after a local minimum. An emission peak blueward of the CO(2,0) absorption band head suggests high-velocity molecular outflow.

The weaker CO absorption in 2018 may be partially filled with circumstellar emission.



An optically thick disk could account for the absorption-line spectrum attributed to the cool companion, as in MWC 623 (Polster et al. 2018).

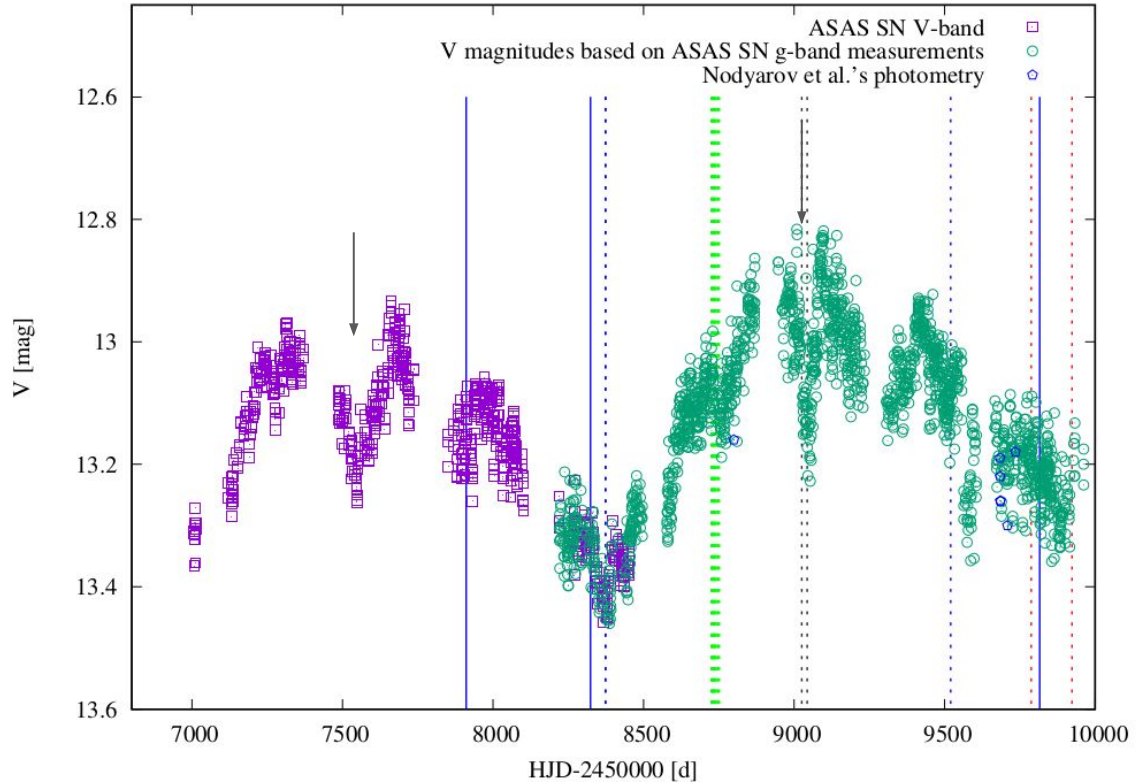


Results and Possible Scenarios...

5) Light Curve and Photometric

Variations: Comparing V-band and g-band magnitudes in the LC curve shows qualitative similarities over 4-year intervals, suggesting a consistent source of variability, possibly from variable CS extinction due to dust clumps (Miroshnichenko et al. 1997, Bouvier et al. 2003).

A simple model insights into the dusty envelope's global properties, featuring various components of optically thin dust, with the closest component at ~ 6 AU. Material orbiting the system at this distance at Keplerian velocity would have a period of ~ 5 years.

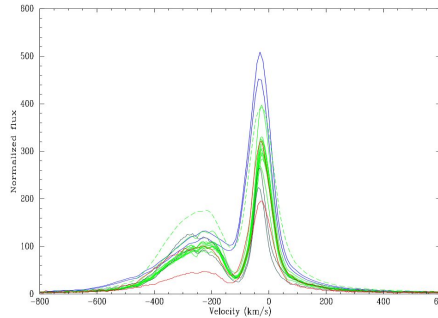
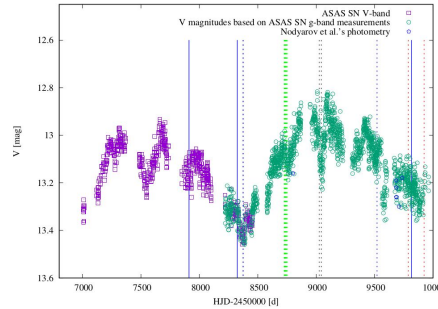


▶ Results and Possible Scenarios...

6) H α Line Variability: Previous studies of MWC 645 lacked reported variations in the V/R ratio of the H α line ($V/R < 1$).

However, we identified variable V/R ratios (from **0.2 to 0.9**, including Nodyarov et al. spectra) and suggested that changes in CS material may be responsible.

Spectroscopic monitoring could provide insights into this variability, that could be related to the rotation of a density perturbation in the disk (Okazaki 1991) or an orbital motion (Kriz & Harmanec, 1975).



7) Brightness and H α Emission Correlation: Dimming in optical brightness correlates with H α emission variations (the smallest V/R ratio and the biggest EW at the minimum of the LC).

Decreasing V/R ratio and increasing EW imply changes in CS material amount, not just increased emission intensity during the LC minimum. The H α line strengthening could be linked to enhanced mass loss or mass ejection events.

The LC of MWC 645 hints at the possibility of periodic behavior. If it were real, the enhancement of the H α line might arise from a process of mass transfer during periastron passage within an eccentric binary system ($P \sim 4$ yr).



Conclusion

In this study of the FS CMa-type object, MWC 645, we have:

- presented IR medium-resolution spectra covering the J-, H-, K-, and L-bands and identified the main spectral features
- reported the presence of CO bands in absorption for the first time
- searched for periodicity in the LC and a possible correlation between its behavior and the spectroscopic optical data
- found that the photometric variations could be explained by variable extinction along the line of sight
- noted that the stellar brightness fading is accompanied by the enhancement of the H α line emission, which might be due to mass ejection events
- fit the observed SED, finding a global picture of the gaseous and dusty structures that could enshroud the binary.

Simultaneous photometric and spectroscopic monitoring, including detailed calculations of the H α line profile, along with consideration of more complex scenarios involving non-conservative mass transfer would be valuable for deepening our study of this complex system and draw a more complete picture of the system's geometry and CS matter structure.



Thank you for your time 😊